


RESEARCH

Open Access



Adipose-derived stem cells therapy effectively attenuates PM_{2.5}-induced lung injury

Junling Gao^{1†}, Juntao Yuan^{1†}, Qun Liu^{2†}, Yuanli Wang¹, Huiwen Wang², Yingjie Chen³, Wenjun Ding¹, Guangju Ji^{2*} and Zhongbing Lu^{1*} 

Abstract

Background: The adverse health effects of fine particulate matter (PM_{2.5}) exposure are associated with marked inflammatory responses. Adipose-derived stem cells (ADSCs) have immunosuppressive effects, and ADSC transplantation could attenuate pulmonary fibrosis in different animal disease models. However, whether ADSCs affect PM_{2.5}-induced lung injury has not been investigated.

Method: C57BL/6 mice were exposed to PM_{2.5} every other day via intratracheal instillation for 4 weeks. After that, the mice received tail vein injections of ADSCs every 2 weeks.

Results: ADSC transplantation significantly attenuated systemic and pulmonary inflammation, cardiac dysfunction, fibrosis, and cell death in PM_{2.5}-exposed mice. RNA-sequencing results and bioinformatic analysis suggested that the downregulated differentially expressed genes (DEGs) were mainly enriched in inflammatory and immune pathways. Moreover, ADSC transplantation attenuated PM_{2.5}-induced cell apoptosis and pyroptosis in the lungs and hearts.

Conclusion: ADSCs protect against PM_{2.5}-induced adverse health effects through attenuating pulmonary inflammation and cell death. Our findings suggest that ADSC transplantation may be a potential therapeutic approach for severe air pollution-associated diseases.

Keywords: Adipose-derived stem cells, PM_{2.5}, inflammation, Pyroptosis

Introduction

Increased airborne fine particulate matter (PM_{2.5}, aerodynamic diameter $\leq 2.5 \mu\text{m}$) concentrations (higher than the World Health Organization air quality guideline level — $10 \mu\text{g}/\text{m}^3$) have been implicated in the development of respiratory and cardiovascular diseases, including chronic obstructive pulmonary disease (COPD) [1],

asthma [2], bronchitis [3], coronary artery disease [4], and atherosclerosis and congestive heart failure [5, 6]. Due to its small size, PM_{2.5} is easily inhaled into the airway and largely deposited in lung alveoli. Although the mechanism underlying the cytotoxicity of PM_{2.5} remains elusive, dysregulation of the inflammatory response is considered a major trigger for cell apoptosis and lung injury [7, 8]. Thus, strategies with anti-inflammatory effects might be effective in attenuating PM_{2.5}-induced disease [9].

It is well documented that adipose-derived mesenchymal stem cells (ADSCs) have multilineage differentiation potential and can differentiate into different cell types,

* Correspondence: gj28@ibp.ac.cn; luzhongbing@ucas.ac.cn

[†]Junling Gao, Juntao Yuan and Qun Liu contributed equally to this work.

²Institute of Biophysics, Chinese Academy of Sciences, Datun Road 15, Chaoyang district, Beijing 100101, China

¹College of Life Science, University of Chinese Academy of Sciences, 19A Yuquanlu, Beijing 100049, China

Full list of author information is available at the end of the article



© The Author(s). 2021 **Open Access** This article is licensed under a Creative Commons Attribution 4.0 International License, which permits use, sharing, adaptation, distribution and reproduction in any medium or format, as long as you give appropriate credit to the original author(s) and the source, provide a link to the Creative Commons licence, and indicate if changes were made. The images or other third party material in this article are included in the article's Creative Commons licence, unless indicated otherwise in a credit line to the material. If material is not included in the article's Creative Commons licence and your intended use is not permitted by statutory regulation or exceeds the permitted use, you will need to obtain permission directly from the copyright holder. To view a copy of this licence, visit <http://creativecommons.org/licenses/by/4.0/>. The Creative Commons Public Domain Dedication waiver (<http://creativecommons.org/publicdomain/zero/1.0/>) applies to the data made available in this article, unless otherwise stated in a credit line to the data.

including adipocytes, osteoblasts, chondrocytes, and hepatocytes [10]. ADSCs can also repair damaged organs and tissues through releasing a variety of paracrine factors and extracellular vesicles (EVs) [11]. These properties render ADSCs attractive therapeutic agents for tissue defects and degenerative diseases. Interestingly, ADSCs have the ability to differentiate into type 2 alveolar epithelial cells [12], and ADSC therapy ameliorates lung injury and fibrosis in a series of pulmonary disorders, including bronchiolitis obliterans [13], idiopathic pulmonary fibrosis [14], and emphysema [12]. Moreover, EVs derived from ADSCs could also alleviate PM_{2.5}-induced lung injury in mice [15]. However, whether ADSCs exert a direct protective effect on PM_{2.5}-induced lung injury remains unclear.

Materials and methods

Reagents

Enzyme-linked immunosorbent assay (ELISA) kits for interleukin 6 (IL-6), IL-1 β , tumor necrosis factor alpha (TNF α), and 3'-nitrotyrosine (3'-NT) were purchased from Abcam PLC (#ab100712, #ab197742, #ab108910, and #ab116691, Cambridge, UK). 4-Hydroxynonenal (4-HNE) ELISA kit was obtained from Donggeboye Biological Technology Co. Ltd. (#DG30947M, Beijing, China). TUNEL staining kits were obtained from the Beyotime Institute of Biotechnology (#C1088 or #C1090, Shanghai, China). Dulbecco's modified Eagle medium/nutrient mixture F-12 (DMEM/F12), fetal bovine serum (FBS), and TRIzol were obtained from Thermo Fisher Scientific Inc. (#11320033, #10099141, #15596026, Waltham, MA, USA). PM_{2.5} was collected using high-volume sampler particle collectors and the morphology, size distribution, and components of the constituents were described in a previous study [16]. All other chemicals made in China were of analytical grade.

ADSCs isolation and characterization

White adipose tissues were harvested from male C57BL/6J mice at the age of 6–8 weeks. After washing two times with ice-cold phosphate buffered saline (PBS), the adipose tissue was mechanically diced, digested, washed, filtered, and centrifuged. The cell pellet was washed with DMEM/F12 one more time and then resuspended in DMEM/F12 supplemented with 10% FBS, and 1% penicillin and streptomycin. Finally, ADSCs were placed in a 10-cm dish and cultured in an incubator at 37 °C with 5% CO₂.

To confirm that ADSCs were successfully isolated from white adipose tissue, the expression of cell surface markers of ADSCs were evaluated by flow cytometry. FITC-conjugated CD44, eFluor® 450-conjugated CD34, and PE-conjugated CD73 and CD90.2 antibodies were purchased from Thermo Fisher Scientific Inc. (#11-

0441-81, #48-0341-80, #12-0731-81, and #12-0903-81). The cells were incubated with an antibody against each of the cell surface markers for 30 min and then subjected to flow cytometry analysis.

To induce differentiation, ADSCs were cultured in adipogenic differentiation medium (DMEM/F12, 10% FBS, 1 μ M insulin, 0.5 μ M dexamethasone, 0.5 mM 3-isobutyl-1-methylxanthine, and 50 μ M indomethacin) or osteogenesis differentiation medium (DMEM/F12, 10% FBS, 5 μ g/ml ascorbic acid, 10 nM dexamethasone, 10 mM β -glycerophosphate, 10 nM 1 α , 25-dihydroxyvitamin D3) for 14 days. After differentiation, the cells were fixed with 10% formalin, washed, and then stained with Oil red O or alizarin red solution.

Experimental animals

Twenty-four 8-week-old male C57BL/6J mice were randomly divided into the control group (8 mice) and PM_{2.5}-exposed group (16 mice). The mice were first treated with 10 μ l PBS (control group) or 10 mg/kg PM_{2.5} in 10 μ l PBS (PM_{2.5}-exposed group) every other day via intratracheal instillation for 4 weeks. Based on a previous report [17], the dose used here was equal to daily exposure to \sim 1500 μ g/m³ PM_{2.5} for 1 month. After PM_{2.5} exposure, mice were randomly assigned to 2 groups, 1 group (8 mice) received ADSCs (2×10^5 cells/mouse) via tail vein injection at the fourth and sixth weeks and the other treated with PBS. At the end of the eighth week, the mice were sacrificed by CO₂ inhalation followed by cervical dislocation. To avoid the errors arising from bias, the group information was blind to the researchers who performed biochemical assays and histological analysis. During the whole experimental period, the mice were housed in cages with corn cob bedding, and were fed commercial mouse chow and distilled water ad libitum. The mice were housed under controlled temperature (22 \pm 2 °C) and relative humidity (40–60%) conditions with a 12-h light/dark cycle. Mice with any abnormalities in skin, hair, bodyweight, and behavior were dropped out from the group.

Histopathological staining

After perfusion with PBS, the mouse lungs were harvested, washed, fixed with formalin, and embedded in paraffin. Lung sections (5 μ m) were stained with hematoxylin and eosin (H&E) stain, a Masson's trichrome stain kit (#G1340, Solarbio Science & Technology Co. LTD, Beijing, China), dihydroethidium (DHE), or a TUNEL staining kit. The neutrophil/Ly-6B is a heavily glycosylated protein expressed on neutrophils [18], while galectin-3 (Gal-3, also called Mac-2 antigen) is a carbohydrate-binding protein expressed on the surface of inflammatory macrophages [19]. To assess neutrophil and macrophage infiltration, lung sections were

also stained with Gal-3 and neutrophil antibodies, respectively. Five mice per group were used for these experiments.

ELISA measurement

Serum TNF α , IL-1 β , and IL-6 levels and pulmonary 3'-NT and 4-HNE levels were determined using commercial ELISA kits according to the manufacturer's instructions. In brief, samples or standard plus antibody cocktail were added to the appropriate wells of the pre-coated microplate. The plate was then incubated overnight at 4 °C with gentle shaking. After washing and adding the chromogen substrates for 10 min, the reactions were terminated by adding the stop solution. The content was calculated according to the standard curve and OD value.

Echocardiographic measurement

After anesthetization with 1.5% isoflurane, the mice were subjected to echocardiographic measurement using a VisualSonics high-resolution Veve 2100 system (Visual Sonics, Toronto, ON, Canada).

RNA isolation and RNA-sequencing

Total RNA was extracted from the lungs (3 mice per group) using TRIzol reagent and RNA quality was measured with an Agilent 2100 bioanalyzer (Thermo Fisher Scientific, MA, USA). The isolated RNA was further purified by DNase I treatment and rRNA removal. Library construction and RNA-sequencing were then performed on a BGISEQ500 platform (BGI-Shenzhen, China).

Read mapping and differentially expressed gene analysis

As described previously [20], the raw data were cleaned with SOAPnuke and trimmomatic software [21], and then the clean reads were mapped to the reference genome (Mus_musculus, GCF_000001635.25_GRCm38.p5) using HISAT [22] or Bowtie 2 [23] software. RESM software [24] was used to obtain the gene expression level and the differential expression of genes (DEGs) between two groups was assessed by DEGseq [25] with the following thresholds: fold change ≥ 2 and adjusted P value ≤ 0.001 . The identified DEGs for each pair were mapped to terms in the Kyoto Encyclopedia of Genes and Genomes (KEGG) database (<http://www.genome.jp/kegg/pathway.html>). The p value was adjusted for the false discovery rate (FDR) to obtain the q -value, and a q -value ≤ 0.05 was considered to indicate significant enrichment.

Gene set enrichment analysis (GSEA) was also performed with the KOBAS 3.0 online tool 1 [26] and Java GSEA2 [27]. An FDR q -value ≤ 0.25 was considered to indicate significant enrichment.

Quantitative real-time PCR and western blotting

A PrimeScript RT reagent kit (#RR036B, TaKaRa, Otsu, Japan) was used for cDNA synthesis. A quantitative real-time polymerase chain reaction (qPCR) assay was performed using the SYBR Premix Ex Taq™ II Kit (#RR820DS, TaKaRa) and the results were normalized to the level of 18 S ribosomal RNA. The primers used in the qPCR assay are listed in Table S1.

Proteins were extracted from the lungs using buffer (50 mM Tris-Cl, 150 mM NaCl, 100 μ g/ml phenylmethylsulfonyl fluoride, protease and phosphatase inhibitor cocktail (#046931124001 and #4906837001, Roche, Basel, Switzerland), and 1% Triton X-100) on ice for 30 min. After centrifugation at 12000 \times g at 4 °C for 20 min, the supernatant was used for western blot analysis. The detail information for antibodies are listed in Table S2.

Data and statistical analysis

All values are expressed as the mean \pm standard deviation (SD). Normal distribution was assessed by the Kolmogorov-Smirnov normality test. The significance of differences was tested using one-way analysis of variance (ANOVA) followed by Fisher's least significant difference test or the Kruskal-Wallis nonparametric test followed by Dunn's test using GraphPad Prism 7 (GraphPad Software Inc., CA, USA). Statistical significance was defined as $p < 0.05$.

Results

Characterization of ADSCs and in vitro differentiation assay

As shown in Figure S1, the isolated ADSCs were positive for CD44 (93.5%), CD73 (97%), and CD90 (95.8%) and negative for CD34 (3.49%). Microscopic observation showed that the cultured ADSCs exhibited a fibroblast-like appearance and formed a monolayer (Figure S2A). To determine the differentiation potential, ADSCs were cultured in adipogenic or osteogenic differentiation induction medium for 14 days. Positive staining with Oil red O and alizarin red indicated that ADSCs could differentiate into adipocytes and osteocytes, respectively (Figure S2B-C).

ADSC transplantation attenuates PM_{2.5}-induced inflammation and pulmonary fibrosis in mice

To investigate the protective effects of ADSCs on PM_{2.5}-induced lung injury and cardiac dysfunction, we treated the PM_{2.5}-exposed mice with ADSCs twice via tail vein injection. The processes of the ADSC transplantation experiment are illustrated in Fig. 1A. At the end of the experimental period, there were significant increases in serum TNF α , IL-1 β , and IL-6 levels in PM_{2.5}-exposed mice, while these increases were diminished in the mice

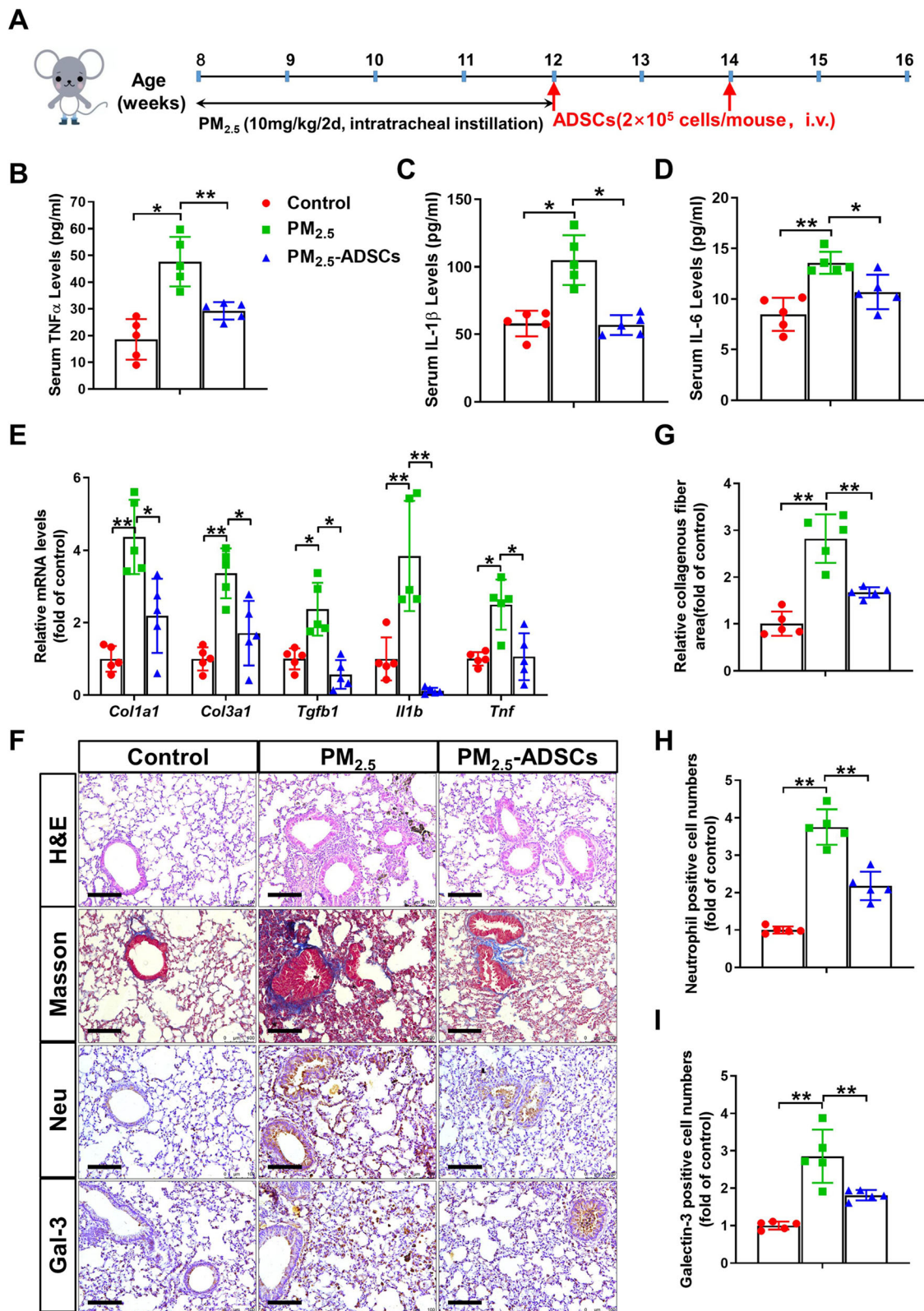


Fig. 1 (See legend on next page.)

(See figure on previous page.)

Fig. 1 Adipose-derived stem cell transplantation alleviated PM_{2.5}-induced inflammation and pulmonary fibrosis. C57BL/6 mice were administered PBS or 10 mg/kg PM_{2.5} every other day via intratracheal instillation for 4 weeks. At the fourth and sixth weeks, some of the PM_{2.5}-exposed mice were treated with adipose-derived stem cells (ADSCs) via tail vein injection (2×10^5 cells/mouse). **A** Schema of the experimental procedure. **B–E** After mice were sacrificed, serum TNF α (**B**), IL-1 β (**C**), and IL-6 (**D**) levels and the mRNA levels of pulmonary inflammatory and fibrotic genes (**E**) were measured. **F** Representative lung sections were stained with hematoxylin and eosin (H&E) stain, Masson's trichrome stain, and antibodies specific for neutrophils and macrophages (galectin-3, Gal-3) (brown staining). Scale bar = 100 μ m. **G–I** The relative collagenous fiber area (**G**) and the numbers of neutrophils (**H**) and Gal-3-positive cells (**I**) were quantified. $N = 5$; the data are presented as the mean \pm SD; asterisk indicates $p < 0.05$; double asterisks indicate $p < 0.01$

that received ADSC transplantation (Fig. 1B–D). Next, we performed qPCR to examine the effects of ADSCs treatment on the mRNA levels of genes related to inflammation and fibrosis. PM_{2.5} exposure caused significant increases in pulmonary collagen I and III, transforming growth factor beta (TGF- β), IL-1 β , and TNF α mRNA levels; however, these increases were significantly attenuated by ADSC transplantation (Fig. 1E). Histopathological analysis of lung sections using H&E and Masson's staining demonstrated that the collapse of alveoli, thickening of airway epithelium, and deposition of collagen in the lungs of PM_{2.5}-exposed mice were attenuated by ADSC treatment (Fig. 1F, G). Immunohistochemical staining with neutrophil and Gal-3 antibodies also showed that PM_{2.5}-induced infiltration of neutrophils and macrophages in the lungs was diminished by ADSC transplantation (Fig. 1F, H, I).

ADSC transplantation prevents PM_{2.5}-induced pulmonary oxidative stress and cell apoptosis in mice

PM_{2.5} exposure significantly increased pulmonary 3'-NT and 4-HNE levels, while these increases in the levels of oxidative stress markers [28] were attenuated by ADSC transplantation (Fig. 2A, B). Moreover, DHE staining revealed that ADSC decreased superoxide levels in PM_{2.5}-exposed lungs (Fig. 2C, D), indicating that ADSC treatment ameliorated PM_{2.5}-induced pulmonary oxidative stress. TUNEL staining showed that ADSC transplantation significantly attenuated the increases in apoptotic cell number in the lungs of PM_{2.5}-exposed mice (Fig. 2C, E). Consistently, the expression of the proapoptotic protein Bax and cleaved caspase-3 was increased, whereas the expression of antiapoptotic protein Bcl-2 was decreased in the lungs of PM_{2.5}-exposed mice. Moreover, PM_{2.5} exposure also decreased superoxide dismutase 1 (SOD1) and peroxiredoxin 4 (PRDX4) protein expression in the lungs. However, the changes in apoptosis and antioxidant related proteins were significantly attenuated by ADSC transplantation (Fig. 2F).

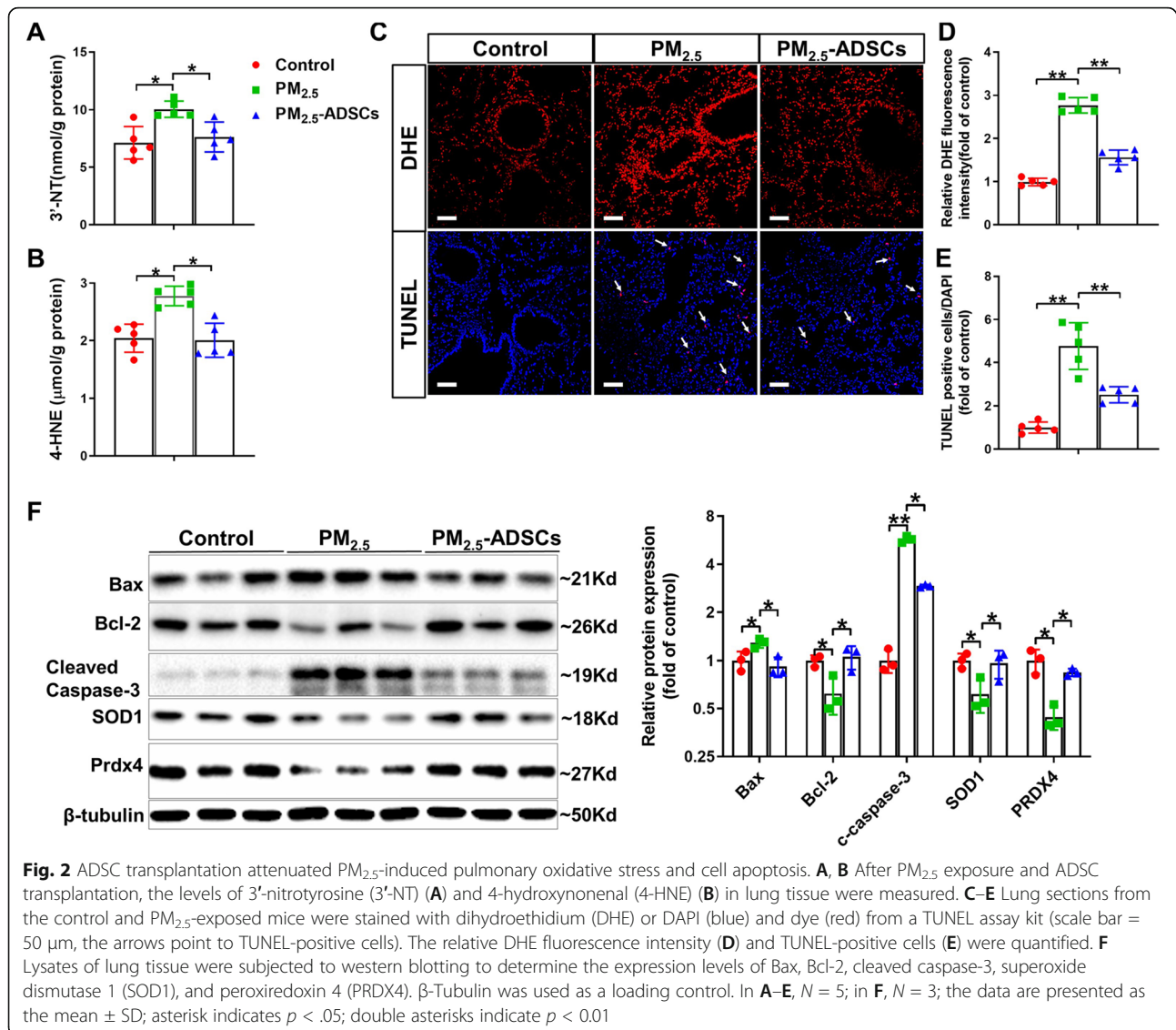
ADSC transplantation has profound effects on the gene expression profile in PM_{2.5}-exposed lungs

To investigate the molecular mechanism by which ADSC transplantation attenuated PM_{2.5}-induced lung

injury in mice, RNA-sequencing was performed to analyze the whole-genome expression profiling changes in these groups. We identified 1217 differential DEGs (866 upregulated and 351 downregulated) in the control group vs PM_{2.5} group and 585 DEGs (423 upregulated and 162 downregulated) in the PM_{2.5} vs PM_{2.5}-ADSC group, and the fold changes of these DEGs were visualized in volcano plots (Fig. 3A). KEGG pathway enrichment analysis demonstrated that the upregulated DEGs in the control group vs PM_{2.5} group were mainly significantly enriched in inflammatory and metabolic pathways, including the PPAR signaling pathway, cytokine-cytokine receptor interaction, chemokine signaling pathway, and adipocytokine signaling pathway (Fig. 3B). Notably, the downregulated DEGs in PM_{2.5} group vs PM_{2.5}-ADSC group were significantly enriched in inflammation and immune pathways, including the cytokine-cytokine receptor interaction, IL-17, chemokine signaling, TNF signaling, and NOD-like receptor signaling pathways (Fig. 3B). To explore the immunosuppressive mechanism of ADSCs in PM_{2.5}-exposed lungs, the expression of the DEGs was visualized in a heatmap (Fig. 3C), which demonstrated that the expression of most of the inflammation-related genes that were upregulated in PM_{2.5}-exposed lungs was repressed by ADSC transplantation. The qPCR results demonstrated that ADSC treatment attenuated the upregulation of *Ccl3*, *Ccl6*, *Csf3r*, *Gdf15*, *Mefv*, *Orm2*, *S100a9*, *Saa3*, and *Tnfrsf19* expression in PM_{2.5}-exposed mice (Fig. 3D).

ADSC transplantation attenuates pyroptosis in PM_{2.5}-exposed lungs

Recent studies have shown that PM_{2.5}-induced pulmonary inflammation is associated with activation of NOD-like receptor protein 3 (NLRP3) and caspase-1 pathway, which can trigger cell pyroptosis [29]. GSEA results showed that the DEGs in the control group vs PM_{2.5} group were significantly enriched in inflammation and immune pathways, including the immune system process, adaptive/innate immune response, inflammatory response, chemotaxis, and immune response (Figure S3). Consistently, the DEGs in the control group vs PM_{2.5} group were also significantly enriched in the pyroptosis pathway (Fig. 4A). To further explore the mechanism

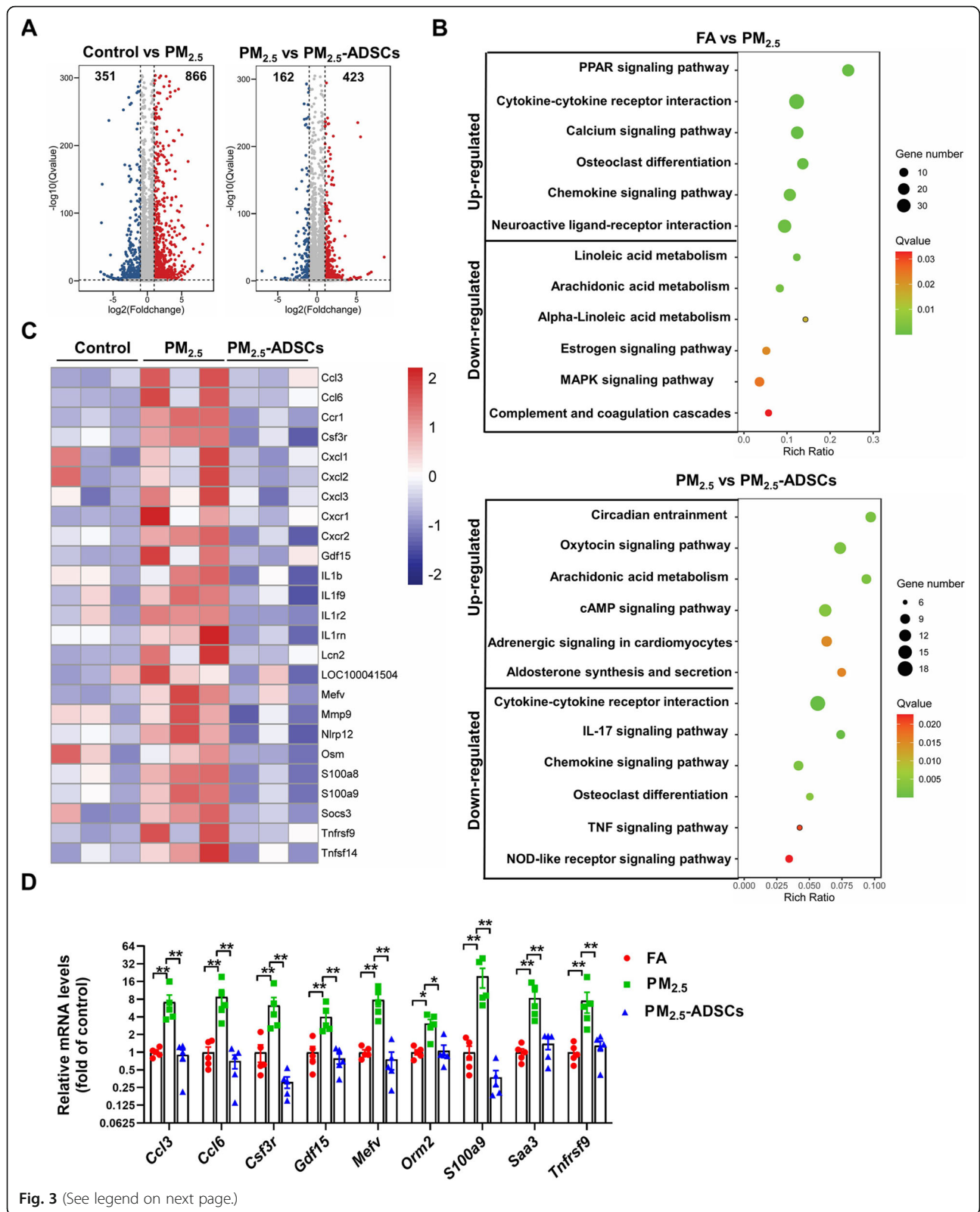


underlying the activation of the pyroptosis pathway in PM_{2.5}-exposed lungs, the expression profiles of genes involved in the pyroptosis pathway were visualized in the heat map (Fig. 4B), which demonstrated that the expression of most of the genes was upregulated in PM_{2.5}-exposed lungs, while the upregulation of the expression of these genes was significantly attenuated by ADSC transplantation. The changes in gene expression were further validated by real-time qPCR, which confirmed that PM_{2.5}-induced upregulation of pulmonary *Aim2*, *Casp4*, *Gsdme*, *IL18rap*, *IL1a*, *Naip2*, and *Nlrp3* gene expression was attenuated by ADSC transplantation (Fig. 4C). Western blotting also showed that PM_{2.5} exposure resulted in significant increases in the expression of NLRP3, IL-1β, cleaved caspase-1, and gasdermin E (GSDME), while the increase in the expression of these

genes was significantly attenuated by ADSC treatment (Fig. 4D).

ADSCs attenuate PM_{2.5}-induced cardiac dysfunction and fibrosis

To determine whether ADSCs could alleviate cardiac dysfunction in PM_{2.5}-exposed mice, we assessed the left ventricular (LV) function. Echocardiographic examination showed that PM_{2.5} exposure significantly decreased ejection fraction (EF) values, while this reduction was attenuated by ADSC treatment (Figure S4A-B). Furthermore, ADSCs also significantly attenuated PM_{2.5}-induced upregulation of myocardial atrial natriuretic peptide (ANP; a marker for cardiac stress) (Figure S4C). As revealed by Masson's staining and TUNEL staining, obvious fibrosis and cardiomyocyte apoptosis occurred



(See figure on previous page.)

Fig. 3 ADSC transplantation affected the gene expression profile in PM_{2.5}-exposed lungs. **A** The fold changes in the expression of differentially expressed genes (DEGs) in the control group vs PM_{2.5} group and the PM_{2.5} group vs PM_{2.5}-ADSC group were visualized in a volcano plot. **B** The advanced bubble chart shows the top 6 significantly enriched KEGG pathways of the up- and downregulated DEGs in the control group vs PM_{2.5} group and the PM_{2.5} group vs PM_{2.5}-ADSC group. **C** The gene expression profiles of the downregulated DEGs in the PM_{2.5} group vs PM_{2.5}-ADSC group that were enriched in inflammatory pathways, as determined by KEGG pathway analysis, are shown in the heat map. **D** To verify the RNA-sequencing results, mRNA levels were measured by real-time qPCR. In **A-C**, *N* = 3; in **D**, *N* = 5; the data are presented as the mean ± SD; asterisk indicates *p* < 0.05; double asterisks indicate *p* < 0.01

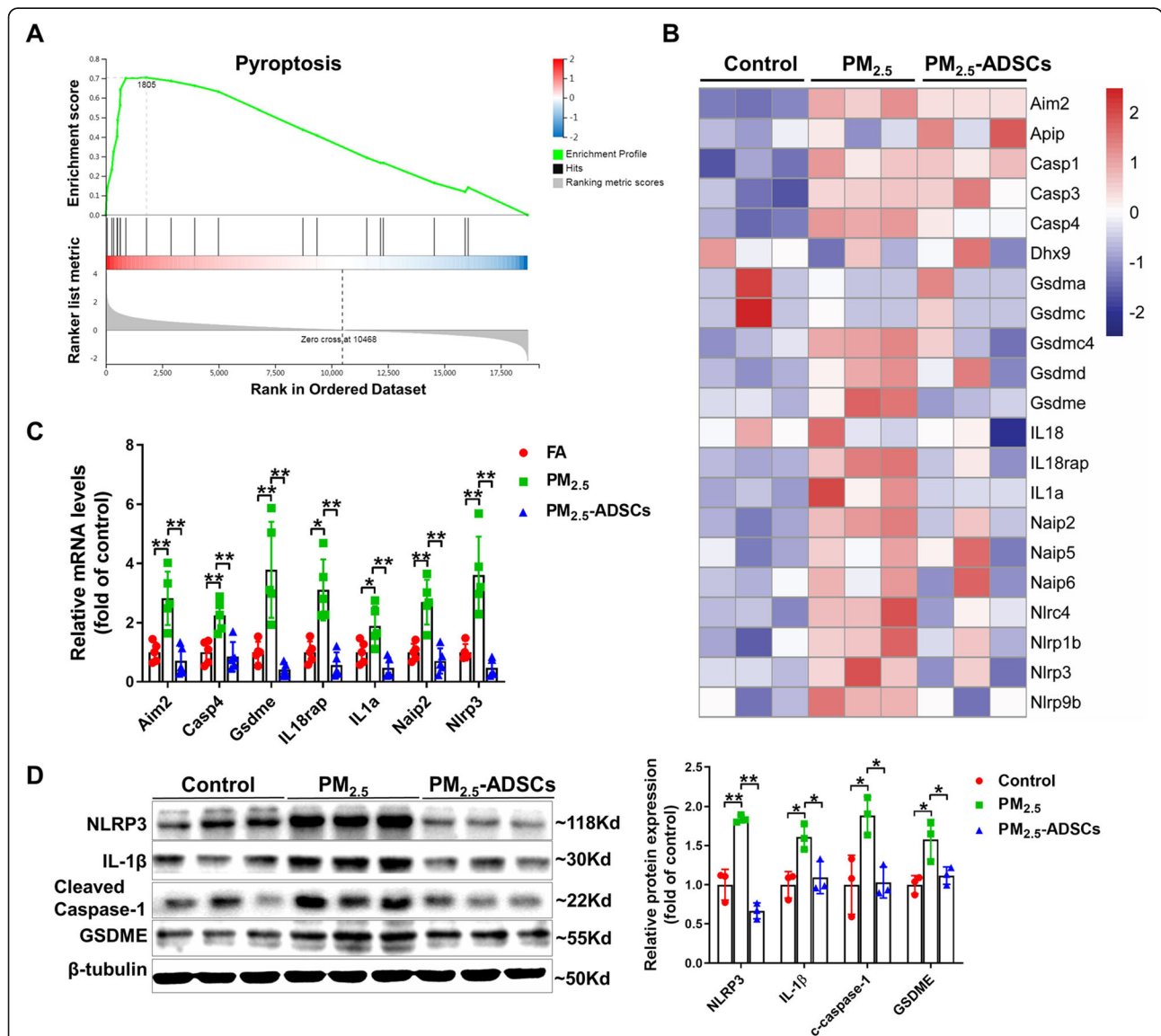


Fig. 4 ADSC transplantation attenuated PM_{2.5}-induced pyroptosis. **A** Gene set enrichment analysis plot showing the DEGs in the control group vs PM_{2.5} group enriched in the pyroptosis pathway. **B** Heat map showing the expression of the genes involved in the pyroptosis process. **C** The mRNA levels of pyroptotic genes were confirmed by qPCR. **D** Lysates of lung tissue were subjected to western blotting to determine the expression levels of NOD-like receptor protein 3 (NLRP3), IL-1β, cleaved caspase-1, and gasdermin E (GSDME). β-Tubulin was used as a loading control. In **C**, *N* = 5; in **D**, *N* = 3; the data are presented as the mean ± SD; asterisk indicates *p* < .05; double asterisks indicate *p* < 0.01

in the hearts of the PM_{2.5}-exposed mice, while the collagenous fibrotic area and apoptotic cell number in these hearts were significantly reduced by ADSC transplantation (Figure S4D-F). Western blotting showed that ADSC transplantation attenuated the PM_{2.5}-induced decrease in Serca2a expression and increases in IL-1 β , cleaved caspase-1, and GSDME expression in the heart (Figure S4G). Together, these results indicated that ADSCs effectively attenuates PM_{2.5}-induced cardiac dysfunction in mice.

Discussion

To the best of our knowledge, the present study provides the first direct evidence that ADSC transplantation is effective in attenuating PM_{2.5}-induced lung injury and cardiac dysfunction. The mechanism underlying the protective effect of ADSCs was associated with the suppression of the inflammatory response and attenuation of cell death.

The finding that ADSC therapy decreased serum TNF α , IL-6, and IL-1 β levels and pulmonary TNF α and IL-1 β mRNA levels in PM_{2.5}-exposed mice suggested that ADSCs protect against PM_{2.5}-induced lung injury, at least partially, by suppressing the inflammatory response. The anti-inflammatory effects of ADSCs have also been observed in different pulmonary disease models, including models of bleomycin-induced interstitial pneumonia [30], lipopolysaccharide-induced pulmonary microvascular barrier damage [31], and ventilator-induced lung injury in rats [32]. Based on previous reports [33, 34], the molecular mechanism underlying the anti-inflammatory actions of ADSCs includes but is not limited to, secretion of immunosuppressive cytokines/EVs [35, 36], inhibition of microphage activation/infiltration [30, 37], a decrease in inflammatory cytokine production, and regulation of T-reg cells [38, 39]. Consistently, we demonstrated here that ADSCs had inhibitory effects on inflammatory cell infiltration and inflammatory pathway activation.

PM_{2.5} exposure can induce apoptosis in different cell lines and apoptosis induction mediated by PM_{2.5} contributes to its adverse health effects [16, 40]. Here, we found that the lung injury and cardiac dysfunction in PM_{2.5}-exposed mice were associated with increases in the number of TUNEL-positive cells and the expression of cleaved caspase-3. It is notably that caspase 3 can also be enrolled in non-apoptotic processes [41]. The proapoptotic role of PM_{2.5} in the lungs was further confirmed by the decrease in Bcl-2/Bax ratio, which is an important inducer for mitochondrial cytochrome c release and caspase activation [42].

There is evidence that PM_{2.5} triggers pyroptosis by activating the NLRP3/caspase-1 signaling pathway in cells and lung tissues [29, 43]. In agreement with previous studies, we also observed that the mRNA expression of

Nlrp3, *Aim2*, *Naip2*, and *Ila*, as well as protein expression of NLRP3, IL-1 β , and cleaved caspase-1, were upregulated in PM_{2.5}-exposed lungs. Pyroptosis can also be regulated by a caspase-1 independent pathway, in which caspase-4, caspase-5, and caspase-11 are apical activators [44]. Moreover, GSDME can induce a switch from caspase-3-mediated apoptosis induced by chemotherapy drugs to pyroptosis when it is highly expressed [45]. In the present study, we found that PM_{2.5} exposure increased the mRNA levels of *Casp4* and *Gsdme* and the protein expression of cleaved caspase-3 and GSDME in the lungs, indicating that PM_{2.5} induced pyroptosis via multiple mechanisms.

The finding that ADSC transplantation attenuated the increases in the number of TUNEL-positive cells, mRNA levels of pyroptosis-related genes and apoptosis- and pyroptosis-related proteins in the lungs and heart suggested that the protective effects of ADSCs against PM_{2.5}-induced lung injury and cardiac dysfunction were associated with inhibition of cell apoptosis and pyroptosis. The antiapoptotic effect of ADSCs has also been observed in silicosis-exposed mice [46], heterotopic tracheal transplantation models [47], and radiation treated rats [48]. However, the antipyroptotic effect of ADSCs has not yet been reported. Considering that pyroptosis plays an important role in the pathogenesis of many respiratory and cardiovascular diseases, it is possible that ADSCs may have more potential clinical applications than expected.

It has been demonstrated that inflammatory chemokines provide axes for effective recruitment of therapeutic adult stem cells to home and engraft in the appropriate injured target tissues [49]. In the present study, we observed that the expression of chemokines, including *Ccl3/6*, *Cxcl1/2/3*, and *Cxcr1/2*, was upregulated in PM_{2.5}-exposed lungs, which may result in a suitable inflammatory microenvironment for the recruitment of ADSCs. As previous studies have proven that ADSCs have the capacity to home and engraft in injured lungs [12, 13, 47], we did not label the ADSCs or track their homing and engraftment during the experimental process. Anyway, this is the limitation of our study. Another limitation of our study is we did not analysis the inflammatory cell infiltration with fluorescence activated cell sorting, which can reveal more information on inflammatory processes.

Conclusion

In summary, our study indicates that ADSCs exhibit anti-inflammatory, anti-fibrotic, and anti-cell death effects in PM_{2.5}-exposed lungs and that the underlying mechanism is associated with their immunosuppressive effects. Our results suggest that ADSC transplantation may be a potential therapeutic approach for air pollution-associated diseases.

Abbreviations

3^h-NT: 3^h-Nitrotyrosine; 4-HNE: 4-Hydroxynonenal; ADSC: Adipose-derived stem cell; ANP: Atrial natriuretic peptide; COPD: Chronic obstructive pulmonary disease; DEGs: Differentially expressed genes; EF: Ejection fraction; EV: Extracellular vesicle; FBS: Fetal bovine serum; GSDME: Gasdermin E; GSEA: Gene set enrichment analysis; H&E: Hematoxylin and eosin; IL: Interleukin; KEGG: Kyoto Encyclopedia of Genes and Genomes; LV: Left ventricular; NLRP3: NOD-like receptor protein 3; PM_{2.5}: Fine particulate matter; PRDX: Peroxiredoxin; TGF- β : Transforming growth factor beta; TNF α : Tumor necrosis factor alpha

Supplementary Information

The online version contains supplementary material available at <https://doi.org/10.1186/s13287-021-02441-3>.

Additional file 1: Table S1. The quantitative real-time PCR primer information. **Table S2.** Detail information for antibodies. **Figure S1.** Flow cytometry analysis of adipose derived stem cells (ADSCs). ADSCs were stained with FITC-conjugated CD44, PE-conjugated CD73 and CD90.2, and eFluor[®] 450-conjugated CD34 antibodies for 30 min and then subjected to flow cytometry analysis. **Figure S2.** Morphology and differentiation potential of ADSCs. (A) Microscopic observation of the cultured ADSCs; (B) ADSCs were cultured in adipogenic differentiation induction medium for 14 days and then stained with oil red O; (C) ADSCs were cultured in osteogenic differentiation induction medium for 14 days and then stained with alizarin red. Scale bar = 200 μ m. **Figure S3.** Gene set enrichment analysis shows the top 6 significant enriched pathways for DEGs of control vs PM_{2.5} group. **Figure S4.** ADSC transplantation attenuated PM_{2.5}-induced cardiac dysfunction. (A, B) After PM_{2.5} exposure with or without ADSC transplantation, echocardiography was used to measure the left ventricular ejection fraction. (C) The mRNA levels of atrial natriuretic peptide (ANP) were measured. (D) Representative heart sections from control and PM_{2.5}-exposed mice were stained with Masson's trichrome stain (scale bar=100 μ m) and a TUNEL assay kit (green) plus DAPI (blue) (scale bar=50 μ m, the arrows point to TUNEL-positive cells). (E, F) The fibrotic area and TUNEL-positive cells were quantified. (G) Lysates of heart tissue were subjected to western blotting for Serca2, IL-1 β , cleaved caspase-1 and GSDME. β -Tubulin was used as a loading control. In Figure A-N, N = 5; in Figure E-F, N = 6, in Figure G, N = 3; * indicates $p < .05$; ** indicates $p < 0.01$. **Figure S5.** Uncropped blot for Fig. 2. **Figure S6.** Uncropped blot for Fig. 4.

Acknowledgements

The authors would like to thank to Fang Li, Xing Zhao, and Hongyan Hu for their kindly help in instrument operation.

Authors' contributions

JG, JY, and QL: experimental design, collection of data, data analysis, and interpretation. YW and HW: collection of data and provision of study material. YC and WD: experimental design and data interpretation. GJ and ZL: conception and design, financial support, manuscript writing, and final approval of the manuscript. The authors read and approved the final manuscript.

Funding

This study was supported by grants from National Natural Science Foundation of China (82070250), National Key R&D Program of China (2019YFA0110400, 2020YFF0304500), and the Fundamental Research Funds for the Central Universities.

Availability of data and materials

The sequencing data for clean reads generated by this study have been deposited in the NCBI Sequence Read Archive (SRA) database (accession number PRJNA727861). All other data generated or analyzed during this study are included in this published article and its supplementary file.

Declarations

Ethics approval and consent to participate

All animal experiments were performed following the guidelines of laboratory animal care (NIH publication no. 85-23, revised 1985) and with approval from the University of Chinese Academy of Sciences Animal Care and Use Committee (no. UCAS-A-20200620).

Consent for publication

Not applicable

Competing interests

The authors declare that they have no competing interests.

Author details

¹College of Life Science, University of Chinese Academy of Sciences, 19A Yuquanlu, Beijing 100049, China. ²Institute of Biophysics, Chinese Academy of Sciences, Datun Road 15, Chaoyang district, Beijing 100101, China. ³Department of Physiology and Biophysics, University of Mississippi Medical Center, Jackson, USA.

Received: 23 March 2021 Accepted: 9 June 2021

Published online: 19 June 2021

References

- Chi R, Chen C, Li H, Pan L, Zhao B, Deng F, et al. Different health effects of indoor- and outdoor-originated PM(2.5) on cardiopulmonary function in COPD patients and healthy elderly adults. *Indoor Air*. 2019;29(2):192–201. <https://doi.org/10.1111/ina.12521>.
- Hendryx M, Luo J, Chojenta C, Byles JE. Air pollution exposures from multiple point sources and risk of incident chronic obstructive pulmonary disease (COPD) and asthma. *Environ Res*. 2019;179(Pt A):108783.
- Ghosh R, Rossner P, Honkova K, Dostal M, Sram RJ, Hertz-Picciotto I. Air pollution and childhood bronchitis: Interaction with xenobiotic, immune regulatory and DNA repair genes. *Environ Int*. 2016;87:94–100. <https://doi.org/10.1016/j.envint.2015.10.002>.
- McGuinn LA, Ward-Caviness CK, Neas LM, Schneider A, Diaz-Sanchez D, Cascio WE, et al. Association between satellite-based estimates of long-term PM2.5 exposure and coronary artery disease. *Environ Res*. 2016;145:9–17. <https://doi.org/10.1016/j.envres.2015.10.026>.
- Hartiala J, Breton CV, Tang WH, Lurmann F, Hazen SL, Gilliland FD, et al. Ambient air pollution is associated with the severity of coronary atherosclerosis and incident myocardial infarction in patients undergoing elective cardiac evaluation. *J Am Heart Assoc*. 2016;5(8):e003947.
- Wang M, Hou ZH, Xu H, Liu Y, Budoff MJ, Szpiro AA, et al. Association of estimated long-term exposure to air pollution and traffic proximity with a marker for coronary atherosclerosis in a nationwide study in China. *JAMA Netw Open*. 2019;2(6):e196553. <https://doi.org/10.1001/jamanetworkopen.2019.6553>.
- Feng S, Gao D, Liao F, Zhou F, Wang X. The health effects of ambient PM2.5 and potential mechanisms. *Ecotoxicol Environ Saf*. 2016;128:67–74. <https://doi.org/10.1016/j.ecoenv.2016.01.030>.
- He M, Ichinose T, Yoshida S, Ito T, He C, Yoshida Y, et al. PM2.5-induced lung inflammation in mice: differences of inflammatory response in macrophages and type II alveolar cells. *J Appl Toxicol*. 2017;37(10):1203–18. <https://doi.org/10.1002/jat.3482>.
- Jia H, Liu Y, Guo D, He W, Zhao L, Xia S. PM2.5-induced pulmonary inflammation via activating of the NLRP3/caspase-1 signaling pathway. *Environ Toxicol*. 2021;36(3):298–307. <https://doi.org/10.1002/tox.23035>.
- Zhang J, Liu Y, Chen Y, Yuan L, Liu H, Wang J, et al. Adipose-derived stem cells: current applications and future directions in the regeneration of multiple tissues. *Stem Cells Int*. 2020;2020:8810813.
- Shukla L, Yuan Y, Shayan R, Greening DW, Karnezis T. Fat therapeutics: the clinical capacity of adipose-derived stem cells and exosomes for human disease and tissue regeneration. *Front Pharmacol*. 2020;11:158. <https://doi.org/10.3389/fphar.2020.00158>.
- Fukui E, Funaki S, Kimura K, Momozane T, Kimura A, Chijimatsu R, et al. Adipose tissue-derived stem cells have the ability to differentiate into alveolar epithelial cells and ameliorate lung injury caused by elastase-induced emphysema in mice. *Stem Cells Int*. 2019;2019:5179172.

13. Lorenzi W, Gonçalves FDC, Schneider N, Silva ÉF, Visioli F, Paz AH, et al. Repeated systemic administration of adipose tissue-derived mesenchymal stem cells prevents tracheal obliteration in a murine model of bronchiolitis obliterans. *Biotechnol Lett.* 2017;39(8):1269–77. <https://doi.org/10.1007/s10529-017-2355-9>.
14. Tashiro J, Elliot SJ, Gerth DJ, Xia X, Pereira-Simon S, Choi R, et al. Therapeutic benefits of mouse, but not old, adipose-derived mesenchymal stem cells in a chronic mouse model of bleomycin-induced pulmonary fibrosis. *Transl Res.* 2015;166(6):554–67. <https://doi.org/10.1016/j.trsl.2015.09.004>.
15. Gao Y, Sun J, Dong C, Zhao M, Hu Y, Jin F. Extracellular vesicles derived from adipose mesenchymal stem cells alleviate PM2.5-induced lung injury and pulmonary fibrosis. *Med Sci Monit.* 2020;26:e922782.
16. Wang H, Shen X, Tian G, Shi X, Huang W, Wu Y, et al. AMPK α 2 deficiency exacerbates long-term PM2.5 exposure-induced lung injury and cardiac dysfunction. *Free Radic Biol Med.* 2018;121:202–14. <https://doi.org/10.1016/j.freeradbiomed.2018.05.008>.
17. Xu Z, Li Z, Liao Z, Gao S, Hua L, Ye X, et al. PM(2.5) induced pulmonary fibrosis in vivo and in vitro. *Ecotoxicol Environ Saf.* 2019;171:112–21. <https://doi.org/10.1016/j.ecoenv.2018.12.061>.
18. Rosas M, Thomas B, Stacey M, Gordon S, Taylor PR. The myeloid 7/4-antigen defines recently generated inflammatory macrophages and is synonymous with Ly-6B. *J Leukoc Biol.* 2010;88(1):169–80. <https://doi.org/10.1189/jlb.0809548>.
19. Dong S, Hughes RC. Macrophage surface glycoproteins binding to galectin-3 (Mac-2-antigen). *Glycoconj J.* 1997;14(2):267–74. <https://doi.org/10.1023/A:1018554124545>.
20. Wang H, Shen X, Liu J, Wu C, Gao J, Zhang Z, et al. The effect of exposure time and concentration of airborne PM(2.5) on lung injury in mice: a transcriptome analysis. *Redox Biol.* 2019;26:101264. <https://doi.org/10.1016/j.redox.2019.101264>.
21. Bolger AM, Lohse M, Usadel B. Trimmomatic: a flexible trimmer for Illumina sequence data. *Bioinformatics (Oxford, England).* 2014;30(15):2114–20.
22. Kim D, Langmead B, Salzberg SL. HISAT: a fast spliced aligner with low memory requirements. *Nat Methods.* 2015;12(4):357–60. <https://doi.org/10.1038/nmeth.3317>.
23. Langmead B, Salzberg SL. Fast gapped-read alignment with Bowtie 2. *Nat Methods.* 2012;9(4):357–9. <https://doi.org/10.1038/nmeth.1923>.
24. Li B, Dewey CN. RSEM: accurate transcript quantification from RNA-Seq data with or without a reference genome. *BMC Bioinformatics.* 2011;12(1):323. <https://doi.org/10.1186/1471-2105-12-323>.
25. Wang L, Feng Z, Wang X, Wang X, Zhang X. DEGseq: an R package for identifying differentially expressed genes from RNA-seq data. *Bioinformatics (Oxford, England).* 2010;26(1):136–8.
26. Xie C, Mao X, Huang J, Ding Y, Wu J, Dong S, et al. KOBAS 2.0: a web server for annotation and identification of enriched pathways and diseases. *Nucleic Acids Res.* 2011;39(Web Server issue):W316–22.
27. Subramanian A, Tamayo P, Mootha VK, Mukherjee S, Ebert BL, Gillette MA, et al. Gene set enrichment analysis: a knowledge-based approach for interpreting genome-wide expression profiles. *Proc Natl Acad Sci U S A.* 2005;102(43):15545–50. <https://doi.org/10.1073/pnas.0506580102>.
28. Syslová K, Böhmová A, Mikoška M, Kuzma M, Pelclová D, Kačer P. Multimarker screening of oxidative stress in aging. *Oxidative Med Cell Longev.* 2014;2014:562860.
29. Zheng R, Tao L, Jian H, Chang Y, Cheng Y, Feng Y, et al. NLRP3 inflammasome activation and lung fibrosis caused by airborne fine particulate matter. *Ecotoxicol Environ Saf.* 2018;163:612–9. <https://doi.org/10.1016/j.ecoenv.2018.07.076>.
30. Kotani T, Masutani R, Suzuka T, Oda K, Makino S, Ii M. Anti-inflammatory and anti-fibrotic effects of intravenous adipose-derived stem cell transplantation in a mouse model of bleomycin-induced interstitial pneumonia. *Sci Rep.* 2017;7(1):14608. <https://doi.org/10.1038/s41598-017-15022-3>.
31. Li C, Pan J, Ye L, Xu H, Wang B, Xu H, et al. Autophagy regulates the therapeutic potential of adipose-derived stem cells in LPS-induced pulmonary microvascular barrier damage. *Cell Death Dis.* 2019;10(11):804. <https://doi.org/10.1038/s41419-019-2037-8>.
32. Liang ZD, Yin XR, Cai DS, Zhou H, Pei L. Autologous transplantation of adipose-derived stromal cells ameliorates ventilator-induced lung injury in rats. *J Transl Med.* 2013;11(1):179. <https://doi.org/10.1186/1479-5876-11-179>.
33. Qi Y, Ma J, Li S, Liu W. Applicability of adipose-derived mesenchymal stem cells in treatment of patients with type 2 diabetes. *Stem Cell Res Ther.* 2019;10(1):274. <https://doi.org/10.1186/s13287-019-1362-2>.
34. Diehl R, Ferrara F, Müller C, Dreyer AY, McLeod DD, Fricke S, et al. Immunosuppression for in vivo research: state-of-the-art protocols and experimental approaches. *Cell Mol Immunol.* 2017;14(2):146–79. <https://doi.org/10.1038/cmi.2016.39>.
35. Xie J, Jones TJ, Feng D, Cook TG, Jester AA, Yi R, et al. Human adipose-derived stem cells suppress elastase-induced murine abdominal aortic inflammation and aneurysm expansion through paracrine factors. *Cell Transplant.* 2017;26(2):173–89. <https://doi.org/10.3727/096368916X692212>.
36. Gao Y, Huang X, Lin H, Zhao M, Liu W, Li W, et al. Adipose mesenchymal stem cell-derived antioxidative extracellular vesicles exhibit anti-oxidative stress and immunomodulatory effects under PM(2.5) exposure. *Toxicology.* 2021;447:152627. <https://doi.org/10.1016/j.tox.2020.152627>.
37. Anderson P, Souza-Moreira L, Morell M, Caro M, O'Valle F, Gonzalez-Rey E, et al. Adipose-derived mesenchymal stromal cells induce immunomodulatory macrophages which protect from experimental colitis and sepsis. *Gut.* 2013;62(8):1131–41. <https://doi.org/10.1136/gutjnl-2012-302152>.
38. Cho KS, Lee JH, Park MK, Park HK, Yu HS, Roh HJ. Prostaglandin E2 and transforming growth factor- β play a critical role in suppression of allergic airway inflammation by adipose-derived stem cells. *PLoS One.* 2015;10(7):e0131813. <https://doi.org/10.1371/journal.pone.0131813>.
39. Cho KS, Park MK, Mun SJ, Park HY, Yu HS, Roh HJ. Indoleamine 2,3-dioxygenase is not a pivotal regulator responsible for suppressing allergic airway inflammation through adipose-derived stem cells. *PLoS One.* 2016;11(11):e0165661. <https://doi.org/10.1371/journal.pone.0165661>.
40. Gao J, Yuan J, Wang Q, Lei T, Shen X, Cui B, et al. Metformin protects against PM(2.5)-induced lung injury and cardiac dysfunction independent of AMP-activated protein kinase α 2. *Redox Biol.* 2020;28:101345. <https://doi.org/10.1016/j.redox.2019.101345>.
41. Wagner DC, Riegelsberger UM, Michalk S, Härtig W, Kranz A, Boltze J. Cleaved caspase-3 expression after experimental stroke exhibits different phenotypes and is predominantly non-apoptotic. *Brain Res.* 2011;1381:237–42. <https://doi.org/10.1016/j.brainres.2011.01.041>.
42. Oltvai ZN, Milliman CL, Korsmeyer SJ. Bcl-2 heterodimerizes in vivo with a conserved homolog, Bax, that accelerates programmed cell death. *Cell.* 1993;74(4):609–19. [https://doi.org/10.1016/0092-8674\(93\)90509-O](https://doi.org/10.1016/0092-8674(93)90509-O).
43. Ding S, Wang H, Wang M, Bai L, Yu P, Wu W. Resveratrol alleviates chronic "real-world" ambient particulate matter-induced lung inflammation and fibrosis by inhibiting NLRP3 inflammasome activation in mice. *Ecotoxicol Environ Saf.* 2019;182:109425. <https://doi.org/10.1016/j.ecoenv.2019.109425>.
44. Man SM, Karki R, Kanneganti TD. Molecular mechanisms and functions of pyroptosis, inflammatory caspases and inflammasomes in infectious diseases. *Immunol Rev.* 2017;277(1):61–75. <https://doi.org/10.1111/immr.12534>.
45. Wang Y, Gao W, Shi X, Ding J, Liu W, He H, et al. Chemotherapy drugs induce pyroptosis through caspase-3 cleavage of a gasdermin. *Nature.* 2017;547(7661):99–103. <https://doi.org/10.1038/nature22393>.
46. Chen S, Cui G, Peng C, Lavin MF, Sun X, Zhang E, et al. Transplantation of adipose-derived mesenchymal stem cells attenuates pulmonary fibrosis of silicosis via anti-inflammatory and anti-apoptosis effects in rats. *Stem Cell Res Ther.* 2018;9(1):110. <https://doi.org/10.1186/s13287-018-0846-9>.
47. Zheng G, Qiu G, Ge M, He J, Huang L, Chen P, et al. Human adipose-derived mesenchymal stem cells alleviate obliterative bronchiolitis in a murine model via IDO. *Respir Res.* 2017;18(1):119. <https://doi.org/10.1186/s12931-017-0599-5>.
48. Jiang X, Jiang X, Qu C, Chang P, Zhang C, Qu Y, et al. Intravenous delivery of adipose-derived mesenchymal stromal cells attenuates acute radiation-induced lung injury in rats. *Cytotherapy.* 2015;17(5):560–70. <https://doi.org/10.1016/j.jcyt.2015.02.011>.
49. Alexeev V, Olavarria J, Bonaldo P, Merlini L, Igoucheva O. Congenital muscular dystrophy-associated inflammatory chemokines provide axes for effective recruitment of therapeutic adult stem cell into muscles. *Stem Cell Res Ther.* 2020;11(1):463. <https://doi.org/10.1186/s13287-020-01979-y>.

Publisher's Note

Springer Nature remains neutral with regard to jurisdictional claims in published maps and institutional affiliations.